SINGLE WALL NANOTUBES: ATOMIC LIKE BEHAVIOUR AND MICROSCOPIC APPROACH

S. Bellucci [1] and P. Onorato [1 2]
[1] *INFN, Laboratori Nazionali di Frascati, P.O. Box 13, 00044 Frascati, Italy.*
[2] *Dipartimento di Scienze Fisiche, Università di Roma Tre, Via della Vasca Navale 84, 00146 Roma, Italy*
(Dated: February 2, 2008)

Recent experiments about the low temperature behaviour of a Single Wall Carbon Nanotube (SWCNT) showed typical Coulomb Blockade (CB) peaks in the zero bias conductance and allowed us to investigate the energy levels of interacting electrons. Other experiments confirmed the theoretical prediction about the crucial role which the long range nature of the Coulomb interaction plays in the correlated electronic transport through a SWCNT with two intramolecular tunneling barriers.

In order to investigate the effects on low dimensional electron systems due to the range of electron electron repulsion, we introduce a model for the interaction which interpolates well between short and long range regimes. Our results could be compared with experimental data obtained in SWCNTs and with those obtained for an ideal vertical Quantum Dot (QD).

For a better understanding of some experimental results we also discuss how defects and doping can break some symmetries of the bandstructure of a SWCNT.

PACS numbers:

I. INTRODUCTION

In the last 20 years progresses in technology allowed the *construction* of several new devices in the range of nanometric dimensions. The known Moore prediction states that the silicon-data density on a chip doubles every 18 months. So we are going toward a new age when the devices in a computer will live in nanometer scale and will be ruled by the Quantum Mechanics laws.

QDs[1,2], which could play a central role within the *quantum computation* as quantum bits (QBIT's)[3,4,5,6,7] have been studied intensively in the last years[8] thanks to the advances in semiconductor technology[9].

QDs are small devices, usually formed in semiconductor heterostructures, with perfectly defined shape and dimensions[8]($< 1\mu m$ in diameter). They contain from one to a few thousand electrons and, because of the small volume available, the electron energies are quantized. The QDs are useful to study a wide range of physical phenomena: from atomic like behaviour[10,11,12] to quantum chaos, to the Quantum Hall Effect (QHE) when a strong transverse magnetic field acts on the device[13,14,15,16].

Recently several scientists proposed a new carbon based technology against the usual silicon one. In this sense the discovery of carbon nanotubes (CNs) in 1991[17] opened a new field of research in the physics at nanoscales[18].

Nanotubes are very intriguing systems and many experiments in the last decade have shown some of their interesting properties[19]. An ideal SWCNT is a hexagonal network of carbon atoms (graphene sheet) that has been rolled up to make a cylinder. The unique electronic properties of CNs are due to their diameter and chiral angle (helicity) parametrized by a roll-up (wrapping) vector (n, m). This vector corresponds to the periodic boundary conditions[20,21] and gives us the dispersion relations of the one-dimensional bands, which link wavevector to energy, straightforwardly from the dispersion relation in a graphene sheet

$$\varepsilon_{m,k} = \pm\gamma\sqrt{1 - 4\cos(\frac{\pi m}{N_b})\cos(\frac{\sqrt{3}k}{2}) + 4\cos^2(\frac{\sqrt{3}k}{2})} \tag{1}$$

where N_b is the number of periods of the hexagonal lattice around the compact dimension (y) of the cylinder. If the SWCNT is not excessively doped all the excitations of angular momentum $m \neq 0$ (corresponding to the transverse motion $k_y = m/R$) cost a huge energy of order ($0.3\ \gamma \approx 1\ eV$), so we may omit all transport bands except for the lowest one. From eq.(1) we obtain two linearly independent Fermi points $\pm\vec{K} \approx \pm\frac{2\pi}{3\sqrt{3}}$ with a right- and a left-moving ($r = R/L = \pm$) branch around each Fermi point (see Fig.(1.c)). These branches are highly linear in the Fermi velocity $v_F \approx 3\gamma/2 \approx 8 \times 10^5$ m/s up to energy scales $E < D \approx 1$ eV. This linear dispersion corresponds to that of a Luttinger Model for 1D electron liquids. Many experiments demonstrated a LL behaviour[22,23,24] in SWCNT[25]with a measurement of the linear temperature dependence of the resistance above a crossover temperature T_c[26].

In nanometric devices, when the thermal energy k_BT is below the energy for adding an additional electron to the device ($\mu_N = E(N) - E(N-1)$), low bias (small V_{sd}) transport is characterized by a current carried by successive discrete charging and discharging of the dot with just one electron.

This phenomenon, known as single electron tunneling (SET) or quantized charge transport, was observed in many experiments in vertical QDs at very small temperature[10,11,12]. In this regime the ground state energy determines strongly the conductance and the period in Coulomb Oscillations (COs). COs correspond to the peaks observed in conductance as a function of

gate potential (V_g) and are crudely described by the CB mechanism[27]: the $N-th$ conductance peak occurs when[15] $\alpha e V_g(N) = \mu_N$ where $\alpha = \frac{C_g}{C_\Sigma}$ is the ratio of the gate capacitance to the total capacitance of the device. The peaks and their shape strongly depend on the temperature as explained by the Beenakker formula for the resonant tunneling conductance[1,27]

$$G(V_g) = G_0 \sum_{q=1}^{\infty} \frac{V_g - \mu_q}{k_B\, T\, \sinh(\frac{V_g-\mu_q}{k_B\, T})} \tag{2}$$

here $\mu_1, ..., \mu_N$ represent the positions of the peaks.

Many experiments showed the peaks in the conductance of QDs and a famous one[11] also showed atomic-like properties of a vertical QD. There the *"addition energy"*, needed to place an extra electron in a semiconductor QD, was defined analogously to the electron affinity for a real atom and was extracted from measurements. The typical addition energy ranges from 10 to $20meV$, while the disappearance of the COs happens above $\approx 50-K$.

The transport in CNs often differs from the quantum CB theory for QDs, because of the one-dimensional nature of the correlated electrons: so we could need a peculiar theory for resonant tunneling in LLs[28,29]. More recently a novel tunneling mechanism[30] was introduced i.e. correlated sequential tunneling (CST), originating from the finite range nature of the Coulomb interaction in SWNTs, in order to replace conventional uncorrelated sequential tunneling. It dominates resonant transport at low temperatures and strong interactions and its prediction agree with experiments[31]. In the experiment a short nanotube segment was created with an addition energy larger than the thermal energy at room temperature (T_R), so that the SET can be observed also at T_R. The conductance was observed to follow a clear power law dependence with decreasing temperature, pointing at a LL behaviour in agreement with Ref.[30].

An interesting observation about the transport in CNs concerns the long-range nature of the Coulomb interaction, which induces dipole-dipole correlations between the tunneling events across the left and right barrier[30]. The crucial question of the range of the interaction in CNs was investigated in different transport regimes e.g. in order to explain the LL behaviour of large Multi Wall[32] and doped[33] CNs.

However many experiments showed COs: e. g. in 1997 Bockrath and coworkers[34] in a rope of CNs below about $10-K$ observed dramatic peaks in the conductance as a function of the gate voltage according the theory of single-electron charging and resonant tunneling through the quantized energy levels of the nanotubes composing the rope[34]. In this regime also a SWCNT behaves as an artificial atom and reveals its shell structure[35](the data were taken at $5mK$). Recent measurements report clean closed nanotube dots showing complete CB[36], which enable us to deduce some properties from the addition energy of SWCNT and discuss the role which the Coulomb interaction could play in a 1D system at small temperatures ($T = 0.1 \div 0.3 - K$).

In this paper we analyze the effects of a long range electron electron interaction in order to determine the addition energy for models chosen by a vertical QD and a SWCNT in the Hartree Fock (HF) approximation.

In section II we introduce microscopic models and corresponding Hamiltonians for SWCNTs and QDs also focusing on a theoretical model for the interaction potential which interpolates between short and long range type interaction. In section III we show our results about the SWCNT and QDs and discuss the effects of asymmetries experimentally observed[36].

II. MICROSCOPIC APPROACH

As showed in eq.(1) near each Fermi point we obtain that the CN could be represented by a typical Luttinger Hamiltonian with linear branches depending on $\overline{k} = k + \alpha K_F$ ($\alpha = \pm 1$ labels the Fermi point). We introduce the operators that create the electrons near one of the Fermi points (label α) belonging to one of the two branches (label ζ corresponding to the sign of k), $\widehat{c}_{\alpha,\overline{k},s}$ and $\widehat{c}^{\dagger}_{\alpha,\overline{k},s}$. In terms of these operators the free and interaction Hamiltonians can be written as

$$H_0 = v_F \sum_{\alpha,\overline{k},s} |\overline{k}| c^{\dagger}_{\alpha,\overline{k},s} c_{\alpha,\overline{k},s} \tag{3}$$

$$H_{int} = \sum_{\{\alpha_i\}} \sum_{k,k',q,s,s'} \left(V^{\{\alpha_i\}}_{k,p,s,s'}(q) c^{\dagger}_{\alpha_1,k+q,s} c^{\dagger}_{\alpha_2,p-q,s'} c_{\alpha_3,p,s'} c_{\alpha_4,k,s} \right) \tag{4}$$

The interaction $V^{\{\alpha_i\}}_{\zeta,\zeta'}(q)$ plays a central role in order to determine the properties of the electron liquid.

A very crucial question is the effective range of the potential and its possible screening in a CN. If we denote by x the longitudinal direction of the tube and y the wrapped one, the single particle wave function for each electron reads

$$\varphi_{\zeta,\alpha}(x) = u_{\zeta,\alpha}(x,y) \frac{e^{i\alpha K_F x} e^{\zeta i k x}}{\sqrt{2\pi L}}$$

where $u_{\zeta,\alpha}(x,y)$ is the appropriate linear combination of the sublattice states $p = \pm$ and L the length of the tube. So we can obtain a simple 1D interaction potential as follows:

$$U^{\zeta,\zeta'}_{\{\alpha_i\}}(x-x') = \int_0^{2\pi R} dy dy'\; u^*_{\zeta\alpha_1}(x,y) u^*_{\zeta'\alpha_2}(x',y') \times U^{\zeta,\zeta'}_0(x - x', y-y')\; u_{\zeta'\alpha_3}(x',y') u_{\zeta\alpha_4}(x,y)\;.$$

These potentials only depend on $x - x'$ and the 1D fermion quantum numbers while $U^{\zeta,\zeta'}_0(x-x', y-y')$ is

obtained from a linear combination of $U(x-x', y-y'+pd\delta_{p,-p'})$ sublattice interactions[37].

Because of the screening of the interaction in CNs and the divergence due to the long range Coulomb interaction in 1D electron systems, it is customary to introduce models, in order to describe the electron electron repulsion. The usual model is the so called Luttinger model, where the electron electron repulsion is assumed to be a constant in the space of momenta, corresponding to a very short range 1D potential (Dirac delta). In order to analyze the effects of long or short range interactions, we introduce a model for the electron electron potential depending on a parameter r, which measures the range of a non singular interaction; it has as limits the very short range potential ($r \to 0$, delta function) and the infinite long range one ($r \to \infty$, constant interaction). So we can conclude that our general interaction model ranges from the very short range one to the infinity long range one and eliminates the divergence of the Coulomb repulsion. In this sense we suppose that our model is good for describing the interaction, if we do not take in account the IR and the UV divergences.

$$U_r(|x-x'|) = U_0\left(\frac{e^{-\frac{|x-x'|}{r}}}{2r} + \frac{r^2}{r^2+|x-x'|^2}\right) . \quad (5)$$

The interaction between two different electrons with momenta k and q follows from the previous formula

$$V(p=|k-q|) = \frac{1}{L^2}\int_0^L dx \int_{-x}^{L-x} e^{ipy}U(y)dy \ .$$

In the limit $L \to \infty$ we can calculate the Fourier transform of eq.(5)

$$V_r(|q-q'|) = V_0\left(\pi r e^{-r|q-q'|} + \frac{1}{1+r^2|q-q'|^2}\right) . \quad (6)$$

The scattering processes are usually classified according to the different electrons involved and the coupling strengths g are often taken as constants. This assumption corresponds to the usual Luttinger model, so we follow this historical scheme, in order to classify the interactions. The backscattering $g_1^{s,s'}$ involves electrons in opposite branches with a large momentum transfer ($q \approx 2k_F$) so $g_1^{s,s'} \approx V(2k_F)$. The forward scattering occurs between electrons in opposite branches g_2 with a small momentum transfer ($q \ll 2k_F$) so $g_2^{s,s'} \approx V(0)$ (or $g_2^{s,s'} \approx V(2\pi/L)$). The forward scattering in the same branch (g_4) involves the pairs ($k \approx k_F, p \approx k_F$) and gives $g_4^{\parallel} \approx V(0) - V(p-k)$ and $g_4^{\perp} \approx V(0)$. Further below, where we discuss the electron electron interaction, we recall the values of the g constants.

Now we want to introduce the analogous model for a semiconductor ideal QD. Usually we describe the dot like a 2D system with an harmonic confinement potential $V(r) = \frac{1}{2}m^*{\omega_d}^2r^2$ according to measurements[11] that demonstrated that vertical QDs have the shape of a disk where the lateral confining potential has a cylindrical symmetry with a rather soft boundary profile. Under this hypothesis the quantum single particle levels depend just on $n = n_+ + n_-$ (the angular momentum is $m = n_+ - n_-$)

$$\varepsilon_n = \hbar\omega_d(n+\frac{1}{2}).$$

The symmetry leads to sets of degenerate single-particle states which form a shell structure: each shell (ε_n) has $2(n+1)$ degenerate states so that the shells are completely filled for $N = 2, 6, 12, 20, etc.$ electrons in the dot (Magic Numbers).

The many body Hamiltonian corresponding to eq.(3) and eq.(4) has the form

$$\hat{H} = \sum_{\alpha}^{\infty}\varepsilon_\alpha\hat{n}_\alpha + \frac{1}{2}\sum_{\alpha,\beta,\gamma,\delta} V_{\alpha,\beta,\gamma,\delta}\ \hat{c}_\alpha^\dagger\hat{c}_\beta^\dagger\hat{c}_\delta\hat{c}_\gamma. \quad (7)$$

Here $\alpha \equiv (n, m, s)$ denotes the single particle state in the single particle energy level ε_α, $\hat{c}_\alpha^\dagger$ creates a particle in the state α and $\hat{n}_\alpha \equiv \hat{c}_\alpha^\dagger\hat{c}_\alpha$ is the occupation number operator. In the following sections we discuss the essential question regarding the electron electron interaction in the dot ($V_{m,m'}^{n,n'}$) and analyze in detail the screening of the effective potential.

III. SINGLE WALL CARBON NANOTUBE: LOW TEMPERATURE BEHAVIOUR AND COULOMB BLOCKADE

Before proceeding with the calculations, we want to point out that the real band structures of measured CNs show some differences with respect to the ideal case discussed (eq.(3)): in order to clarify this point we shortly discuss the model and the results of two recent experiments.

To begin with, we have to introduce a quantization due to the finite longitudinal size of the tube (L) in the dispersion relation eq.(1). The longitudinal quantization introduces a parameter which also gives a thermal limit for the Atomic Like behaviour: in fact k wavevectors have to be taken as a continuum if K_BT is as a critical value $E_c = v_F\frac{h}{L}$ and as a discrete set if the temperature is below (or near) E_c.

After the quantization we obtain shells with an 8-fold degeneracy due to σ (spin symmetry), α ($K, -K$ lattice symmetry), ζ ($(k-K), (K-k)$ Luttinger symmetry).

Recent experiments do not support such a high symmetry and different hypotheses were formulated in order to explain this discrepancy.

According to Cobden and Nygard[36] *"the sole orbital symmetry is a two-fold one, corresponding to a K-K' subband degeneracy and resulting from the equivalence of the two atoms in the primitive cell of graphene structure"*. Experimentally one can answer this question by observing the grouping of the peaks in plots of the conductance

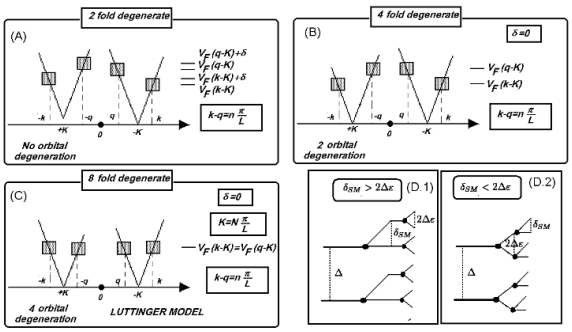

FIG. 1: The dispersion relation and the quantized levels. The boxes in figure represent energy levels and can be filled by a pair of electrons with opposite spins. a) The general case without any degeneracy. b) The 4-fold degeneracy case with $\delta_{SM} = 0$. c) The 8-fold degeneracy case. d) Differences in the splitting due to the comparison between δ_{SM} and $\Delta\varepsilon$.

versus the gate potential. However in the experiment no four-fold grouping was observed because degeneracy was lifted by a mixing between states due either to defects or to the contacts.

A different experiment[38] displays conductance peaks in clusters of four, indicating that there is a four fold degeneracy. In ref.[38] two different shell filling models are put forward: the first one, when the subband mismatch dominates, predicts that the spin in the SWCNT oscillates between $S = 0$ and $S = 1/2$.

In order to take into account the strong asymmetries measured experimentally we modify the dispersion relation. A first correction has to be introduced because of the *"longitudinal incommensurability"*: in general K is not a multiple of π/L so $K = (N + \delta N)\frac{\pi}{L}$ with $\delta N < 1$ and the energy shift is $\Delta\varepsilon = v_F \frac{h\delta N}{L}$. A second correction is due to the subband mismatch (δ_{SM}). The single electron energy levels are

$$\varepsilon_{l,\sigma,p} = \hbar v_F |l\frac{\pi}{L} + pK| + \frac{(1-p)}{2}\delta_{SM} \qquad (8)$$

where $p = \pm 1$.

Each choice of parameters gives a different degeneracy for the quantum levels: the 8-fold degeneracy corresponds to $\delta_{SM} = 0$ and $K = n\frac{\pi}{L}$; the 4-fold degeneracy is found if we put just $\delta_{SM} = 0$ and the 2 fold degeneracy represents the general case (see Fig.(1)).

A. High band structure symmetry: damping in the addition energy oscillations

In the discussion which follows we analyze the effects of the range of the Coulomb interaction in a simplified system with just two linear symmetric branches. In this model each shell is filled by 4 electrons with opposite momenta and spin. We can look for the conservation laws of our Hamiltonian and find the Number of electrons (N), the Energy, the total linear momentum $K = 0$ and the spin $S, S_z = 0$.

The Fermi sea corresponds to the state where all the shells with energy below the Fermi energy ($E_F = v_F n_F h/L$) are totally filled ($N_F = 4n_F$). This state will be our ground state $\Psi_0(N_F)$ and this is true also for interacting electrons in absence of correlation (i.e. in the HF approximation).

The effects of correlation will be discussed in a further article, here we have to explain the range of validity of our approximation. The first thing to consider is the interaction strength $g \approx V(0) - V(2k_F)$ compared to the kinetic energy $v_F h/L$. The HF approximation is valid if $g \ll v_F h/L$. However also the temperature plays a central role, in fact if the temperature increases we have to take into account more excited states (a sort of thermal cut-off corresponds to the energy $k_B T$) so if we are at a very low temperature we can assume the Fermi sea state as the ground state.

At this point we are able to calculate the *addition energy (E_N^A)* following the *Aufbau* sequence explained in Appendix A. E_N^A has a maximum for some numbers $4, 8, 12, ..4n$ (n integer) due to the shell filling. The shells are filled sequentially and Hund's rule determines whether a spin-down or a spin-up electron is added so that the singlet ($S = 0$) energy for a $4n + 2$ system is always greater than the triplet ($S = 1$) one. Obviously this is an effect of interaction and is quite different for the long and short range models.

As we show in Fig.(2) the oscillations due to Hund's rule correspond to the short range potential while the attenuation of these oscillations when the number of electrons in the 1D system increases is due to the long range interaction. So we can draw the following conclusions:

◇ The 4−fold degenerate model predicts oscillations in the addition energy due to the Hund's rule quite similar to the ones observed in QDs.

◇ The oscillations periodicity is 4 for this model (8 for a system with two Fermi points)

◇ The oscillations amplitude is due to an exchange term (proportional to the short range interaction).

◇ The effect of a long range interaction is a damping of the oscillations when the number of electrons in the system increases.

The model with 8-fold degeneracy (see Fig.(1)) has two basic symmetries: $k \to -k$, $KL/\pi = N_K$ and usually the interaction between the electrons with momenta near K and the ones with momenta near $-K$ is very small so that we have two independent 4-fold degenerate Hamiltonians ($n_F = N/4 << N_K$).

B. Asymmetric model

Now we have to analyze models without symmetries by using eq.(8) in the HF approximation.

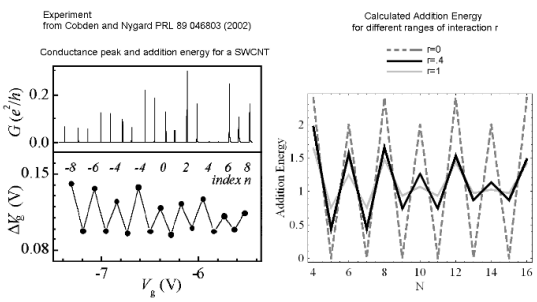

FIG. 2: On the right we show analytical Aufbau results for the addition energy versus the number of electrons of a 4-fold degeneracy model corresponding to different values of the range r ($r = 0$ dark gray dashed line, $r = 0.4$ black line, $r = 1$ gray line). We show how the damping in the oscillations is due to a long range interaction while it does not appear for a $r = 0$ model. Our predictions can be compared with the measured addition energy in the Cobden Nygard experiment displayed on the left.

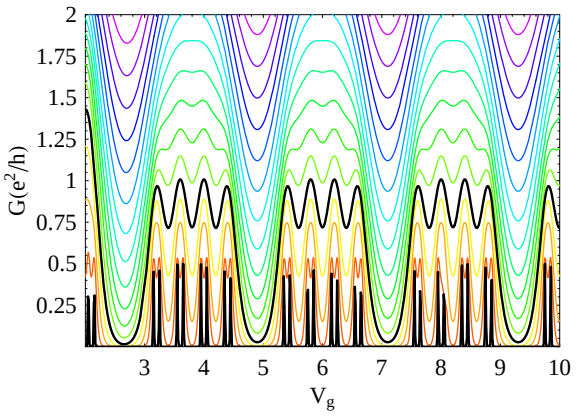

FIG. 3: The asymmetric model calculation for the COs (conductance vs. gate voltage) at different temperatures expressed in terms of Δ calculated following the classical CB theory. Theoretical calculations show that the fine structure peaks are appreciable just for very low temperatures.

In order to introduce the electron electron interaction, we take in account just two ($g^{\parallel}$ and $g^{\perp}$) of the many constants that we introduced in section II from eq.(6). For allowing to compare easily our results with those in ref.[39], as well as with experiments, we give our results in terms of V_0 and J, obtained as a linear combination of the g constants.

Following the usual method, in order to calculate the energy levels, we put

$$g^{\parallel} = V_0 - J \; ; \quad g^{\perp} = V_0 \; ; \quad \Delta = \frac{v_F h}{2L}, \; ; \quad \Delta\varepsilon = \delta N \frac{v_F h}{L}.$$

Here $\Delta\varepsilon$ is the incommensurability shift ($\Delta\varepsilon < 0.5\Delta$). The single particle energies have a different structure for $\delta_{SM} > 2\Delta\varepsilon$ and $\delta_{SM} < 2\Delta\varepsilon$, as we show in Fig.(1.d).

From the experimental data[38] we obtain

$$V_0 \approx U + \delta U + J_{exp} \approx .42 \quad and \quad J \approx J_{exp} - 2\delta U \approx .05$$

where we assume $U = .22$, $\delta U = .05$ and $J_{exp} = .15$ in units of Δ. Under these conditions J is always less than the level spacing.

Now we can write the Hamiltonian of the nanotube depending on these parameters[39]

$$H = \sum_{n,\zeta,p,s} \varepsilon_{n,\zeta,p} \hat{n}_{n,\zeta,p,s} + V_0 \frac{N(N+1)}{2} - J \sum_{n,\zeta,p,s} \sum_{n`,\zeta`,p`,s} \delta_{s,s`} \hat{n}_{n,\zeta,p,s} \hat{n}_{n,\zeta,p,s} \tag{9}$$

Since J is less than the level spacing the energy that we need, in order to add one electron is ε, corresponding to the lowest empty energy level with an interaction energy

$$V_0 \frac{N(N-1)}{2} - J\frac{N-1}{2} \quad for \quad odd \quad N$$
$$V_0 \frac{N(N-1)}{2} - J\frac{N}{2} \quad for \quad even \quad N.$$

Starting from the Hamiltonian eq.(9) we are able to calculate the ground states of the many electron system for various N.

Our results can be compared to the experimental results where strong asymmetries were found. In Fig.(3) we show the peaks corresponding to an asymmetric model to which we apply the classical theory of CB, i.e. eq.(2). The fine structure with 8 periodicity is destroyed by thermal effects: it is appreciable at smaller temperatures (we assume about $T_s \approx 300 \div 500mK$ for a Nanotube's length of about $100 \div 300nm$) and disappears at a temperature $T \approx 4T_s$ ($T \approx 1.2 \div 2.0K$ see ref.[38]) where just a 4 periodicity appears. So, we conclude that we should not be able to observe any small asymmetries effects if the temperature increases. Fig.(3) shows how the Coulomb peaks in the conductance disappear when the temperature increases. In a future article we will show how the end of the CB regime corresponds to the beginning of another one.

Now we want point out the limits of the approach used in the previous sections: the HF approximation ignores the effects of correlation. This corresponds to the Fermi Liquid theory and gives good results just if we can assume that the interaction is smaller than the kinetic energy ($g \ll \hbar v_F$).

Thermal effects are quite important too. In fact the temperature appears in the Beennaker formula and is responsible of the disappearance of the Coulomb peaks. However, if the temperature is higher for a SWCNT, it is the same Beennaker formula which fails, because the HF calculated energy levels are very different from the real energy levels of the electron system. When T is above a critical value

$$T_c = \frac{v_F h}{L k_B} \tag{10}$$

we cannot consider the Fermi sea as the ground state of the electron system in a SWCNT because some other

states with the same linear momentum $K = 0$ and different kinetic energy are also available for the system. So for temperatures above the critical value we have to take into account strong effects of correlation.

C. Quantum Dots and Long Range Interactions

As we did for a SWCNT we calculate the addition energy of a QD in the HF approximation.

As we discussed in section II peaks and oscillations in the measured addition energy correspond to the ones of a shell structure for a two-dimensional harmonic potential. However, in experiments[11], high values of the addition energy are observed also for $N = 4, 9, 16, etc.$ corresponding to those values of the Number of electrons in the dot for which, respectively, the second, third and fourth shells are half filled with parallel spins in accordance with Hund's rule. Half filled shells correspond to a maximum spin state, which has a relatively low energy[10,11].

We compare a non-interacting model with models that include Coulomb interactions especially the exchange term. In Fig.(4) we plot the calculated addition energy as a function of the number of electrons in the following three different cases:

◇ The non-interacting model gives us just the peaks corresponding to the Magic Numbers.

◇ The model with constant parameters ($g^{\parallel}$ and $g^{\perp}$) corresponds to a short range interaction (Dirac δ). The Coulomb exchange term in HF gives the Hund's rule and allows us to explain the oscillations in the addition energy as we show in Fig.(4.a).

◇ The third model is the long range interaction one, where we introduce two measured effects that are both due to the long range Coulomb interaction. The first one is due to the classical capacitive effect shown in Fig.(4.b and c) as a continuous line. The second one is due to the long range correction to Coulomb exchange.

We could compare these results to the experiments (e.g. see ref[11]).

IV. CONCLUSIONS

In this work we have analyzed some properties of a 1D (SWCNT) and 0D-2D (QDs) electron systems by introducing a model of interaction capable of interpolating from short to long range, in order to analyze the effects of the long range component of electron electron interactions.

We have obtained that a damping in the oscillations of the addition energy could be predicted for these models corresponding to the presence of a long range interaction. The results can be compared to the experiments and we discussed the limits for the experimental observation of our predictions in SWCNT. In fact the breakdown of the Fermi Liquid opens different regimes where the tunneling has to be considered as resonant tunneling in LLs[28,29].

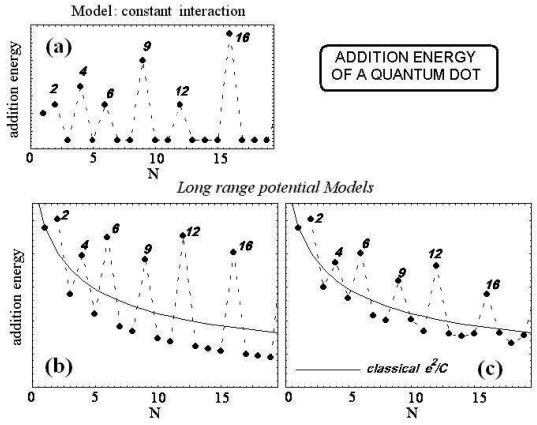

FIG. 4: In a),b),c) results from three different models of interacting electrons in QDs are displayed. The simple HF calculation in a) has to be corrected because it does not take into account the classical capacitive effect. In order to determine it we recall that the electrons in the dot give a charge droplet of radius R_D not fixed, so that we can approximate it with a disk of capacitance $C = C_0 R_D$. The value of R_D can be calculated from classical equations, $R_D \propto \sqrt{N+1}$. So we add the classical term to the damped oscillations due to long range affected Coulomb exchange and obtain the b) and c) plot in the figure.

So we have to limit ourselves to describing an electron system only when it is uncorrelated. This is true only if the interaction strength is small ($g << v_F h/L$)[40] and the temperature is below the critical value T_c (see eq.10).

Acknowledgments

This work was partially supported by the Italian Research Ministry MIUR, National Interest Program, under grant COFIN 2002022534.

APPENDIX A: AUFBAU AND ENERGIES FOR THE 4-FOLD DEGENERATE MODEL

We start by taking into account that each electron in the $|k| > k_F$ state interacts with all the electrons in the filled shells with k below k_F so that we can have the following two (or four) Σ_{HF} terms:

$$\Sigma_{s,\sigma}(k_F, k) = \sum_{p=1}^{k_F} U^{s,\sigma}_{|k-p|} + \sum_{p=-1}^{-k_F} U^{s,\sigma}_{|k-p|}$$

If we introduce $n_F = \frac{L}{\pi} k_F$ and consider the direct term of the interaction, we conclude that

$$\Sigma_{\uparrow\downarrow}(k_F,k) = 2V_0 n_F$$
$$\Sigma_{\uparrow\uparrow}(k_F,k) = V_0\left(2n_F - \sum_{p=-k_F}^{k_F} J_{|p-k|}(1-\delta_{p,0})\right)$$

Obviously if we add an electron in the lowest energy empty shell we obtain $\Sigma(k_F, k_F + \frac{\pi}{L}) \approx V_0\left(4n_F - \sum_{p=\frac{\pi}{L}}^{2k_F+\frac{\pi}{L}} J_p\right)$.

For each shell we can consider the internal interaction energy as

$$w(k) = 2V_0(3 - J_{2k}) \qquad W(k_F) = \sum_{p=\frac{\pi}{L}}^{k_F} w(p)$$

so that the total energy of a system with n_F filled shells reads

$$E_{4n_F} = 2v_F n_F(n_F+1) + W(k_F) + 4\sum_{p=0}^{k_F-\frac{\pi}{L}} \Sigma(p, p+\frac{\pi}{L})$$

a. Energy levels

When we add one by one the electrons to the $4n_F$-system we obtain

$$\mu_{4n_F+1} = \hbar v_F\left(k_F+\frac{\pi}{L}\right) + \Sigma(k_F, k_F+\frac{\pi}{L})$$
$$\mu_{4n_F+2} = \hbar v_F\left(k_F+\frac{\pi}{L}\right) + \Sigma(k_F, k_F+\frac{\pi}{L}) + U_0(1-\gamma)$$
$$\mu_{4n_F+3} = \hbar v_F\left(k_F+\frac{\pi}{L}\right) + \Sigma(k_F, k_F+\frac{\pi}{L}) + 2U_0$$
$$\mu_{4n_F+4} = \hbar v_F\left(k_F+\frac{\pi}{L}\right) + \Sigma(k_F, k_F+\frac{\pi}{L}) + U_0(3-\gamma)$$
$$\mu_{4n_F+5} = \hbar v_F\left(k_F+2\frac{\pi}{L}\right) + \Sigma(k_F+\frac{\pi}{L}, k_F+2\frac{\pi}{L})$$

where $\mu_{N+1} = E_{N+1} - E_N$ and $\gamma = \frac{J_{2k_F}}{U_0}$

The addition energy is also calculated as $E^A_{N+1} = \mu_{N+2} - \mu_{N+1}$ so that

$$E^A_{4n_F+1} = U_0(1-\gamma) \qquad E^A_{4n_F+2} = U_0(1+\gamma)$$
$$E^A_{4n_F+3} = U_0(1-\gamma) \qquad E^A_{4n_F+4} = U_0(1+\gamma) + \left(\frac{\hbar v_F \pi}{L}\right)$$

[1] L.P. Kouwenhoven, C.M. Marcus, P.L. McEuen, S. Tarucha, R.M. Westervelt, and N.S. Wingreen, in *Mesoscopic Electron Transport*, (Kluwer, Dordrecht, The Netherlands, 1997).

[2] P.L. McEuen, Science **278**, 1729 (1997).

[3] *Spintronics and Quantum dots for Quantum Computing and Quantum Communication* G. Burkard, H.A. Engel and D. Loss in Experimental proposal for Quantum Computation eds. H.-K. Lo and S. Braunstein.

[4] B.E. Kane, Nature (London) **393**, 133 (1998); G.A. Prinz, Science **282**, 1660 (1998).

[5] D.P. DiVincenzo, D. Bacon, J. Kempe, G. Burkard and K.B. Whaley, Nature (London) **408**, 339 (2000); D. Loss and D.P. DiVincenzo Phys. Rev. A **57**, 120 (1998) ; D.P. DiVincenzo, Science **269**, 255 (1995).

[6] S.A. Wolf *et al.*, Science **294**, 1488 (2001).

[7] S. Datta and B. Das, Appl. Phys. Lett. **56**, 665 (1990).

[8] E.B. Foxman *et al.*, Phys. Rev. B **47**, 10020 (1993); R.C. Ashoori, Nature **379**, 413 (1996).

[9] T.J. Thornton, Rep. Prog. Phys. **57** (1994).

[10] L.P. Kouwenhoven and C. Marcus, Physics World, June 1999.

[11] S. Tarucha, D.G. Austing, T. Honda, R.J. van der Hage, L.P. Kouwenhoven, Phys. Rev. Lett. **77**, 3613 (1996).

[12] T.H. Oosterkamp, J.W. Jansen, L.P. Kouwenhoven, D.G. Austing, T. Honda, S. Tarucha, Phys. Rev. Lett. **82**, 2931 (1999).

[13] O. Klein, C. de C. Chamon, D. Tang, D.M.Abusch-Magder, U. Meirav, X.-G.Wen, and M.A.Kastner and S.J. Wind Phys. Rev. Lett. **74**, 785 (1995).

[14] O. Klein, D. Goldhaber-Gordon, C. de C. Chamon and M.A.Kastner Phys. Rev. B **53**, 4221 (1996).

[15] O. Klein et al. In *Quantum Transport in Semiconductor Submicron Structures* ed. Kramer (1996).

[16] A.H. Mac Donald, S.-R. E. Yang and M.D. Johnson Phys. Rev. Lett. **71**, 3194 (1993); S.-R. E. Yang, A.H. Mac Donald and M.D. Johnson, Aust. J. Phys. **46**, 345 (1993).

[17] S. Iijima, Nature **354**, 56 (1991).

[18] P.L. McEuen, Nature **393**, 15 (1998).

[19] T.W. Ebbesen, Physics Today **49 (6)**, 26 (1996); R.E. Smalley, Rev. Mod. Phys. **69**, 723 (1997); P.G. Collins, A. Zettl, H. Bando, A. Thess, and R.E. Smalley, Science **278**, 100 (1997).

[20] J. González, F. Guinea and M. A. H. Vozmediano, Nucl. Phys. B **406**, 771 (1993).

[21] R. Saito, M. Fujita, G. Dresselhaus, and M. S. Dresselhaus, Phys. Rev. B **46**, 1804 (1992).

[22] Z. Yao, H. W. Postma, L. Balents, and C. Dekker, Nature London **402**, 273 (1999).

[23] C. Kane, L. Balents, and M. P. A. Fisher, Phys. Rev. Lett. **79**, 5086 (1997).

[24] M. Bockrath, D. H. Cobden, J. Lu, A. G. Rinzler, R. E. Smalley,L. Balents, and P. L. McEuen, Nature London **397**, 598 (1999).

[25] M. Bockrath, D. H. Cobden, J. Lu, A. G. Rinzler, R. E. Smalley, L. Balents and P. L. McEuen, Nature **397**, 598 (1999).

[26] J. E. Fischer, H. Dai, A. Thess, R. Lee, N. M. Hanjani, D. L. Dehaas, and R. E. Smalley, Phys. Rev. B **55**, R4921 (1997).

[27] C. Beenakker, Phys. Rev. B **44**, 1646 (1991).

[28] C. L. Kane and M. P. A. Fisher, Phys. Rev. B **46** , 15233 (1992); A. Furusaki and N. Nagaosa, Phys. Rev. B **47** , 3827 (1993); A. Furusaki, Phys. Rev. B **57** , 7141 (1998); A. Braggio et al., Europhys. Lett. **50** , 236 (2000)

[29] Yu. V. Nazarov and L. I. Glazman Phys. Rev. Lett. **91**, 126804 (2003).

[30] M. Thorwart, M. Grifoni, G. Cuniberti, H. W. Ch. Postma and C. Dekker, Phys. Rev. Lett. **89**, 196402 (2002).

[31] H. W. Ch. Postma *et al.*, Science **293** , 76 (2001).

[32] S. Bellucci and J. González, Eur. Phys. J. B **18**, 3 (2000); S. Bellucci and J. González, Phys. Rev. B **64**, 201106(R) (2001).

[33] S. Bellucci, J. González and P. Onorato, Nucl. Phys. B **633**, 605 (2003); S. Bellucci, J. González and P. Onorato, Phys. Rev. B **69**, 085404 (2004).

[34] M. Bockrath, D. H. Cobden, P. L. McEuen, N.G. Chopra, A. Zettl, A. Thess and R. E. Smalley, Science **275**, 1922 (1997).

[35] S. J. Tans, M. H. Devoret, R. J. A. Groeneveld, C. Dekker , Nature **386**, 474 (1997).

[36] D.H. Cobden and J. Nygard , Phys. Rev. Lett. **89**, 46803 (2002).

[37] R. Egger and A. O. Gogolin, Eur. Phys. J. B **3**, 281 (1998).

[38] W. Liang M. Bockrath and H. Park, Phys. Rev. Lett. **88**, 126801 (2002).

[39] Y. Oreg, K. Byczuk, and B. I. Halperin, Phys. Rev. Lett. **85**, 365 (2000).

[40] This also corresponds to a long Nanotube so we cannot apply it to the experiments in ref[31] which concern short Nanotubes.